

Longitudinal-vertical integrated sliding mode controller for distributed electric vehicles

Yan MA^{1,2}, Jinyang ZHAO², Haiyan ZHAO^{1,2*}, Hong CHEN^{1,2} & Tielong SHEN³

¹State Key Laboratory of Automotive Simulation and Control, Jilin University, Changchun 130000, China;

²Department of Control Science and Engineering, Jilin University, Changchun 130000, China;

³Department of Engineering and Applied Sciences, Sophia University, Tokyo 102-8554, Japan

Received 22 December 2018/Accepted 31 January 2019/Published online 17 April 2020

Citation Ma Y, Zhao J Y, Zhao H Y, et al. Longitudinal-vertical integrated sliding mode controller for distributed electric vehicles. *Sci China Inf Sci*, 2020, 63(11): 219201, <https://doi.org/10.1007/s11432-018-9810-4>

Dear editor,

In the recent years, with the advancements in vehicular technology, the vehicle dynamics control has attracted considerable research attention [1,2]. Many active stability control systems have played a significant role in the chassis control of electric vehicles (EV), promising upgraded, more secure, and intelligent versions. In most automotive control design approaches, the traction control system and active suspension system optimize and control the longitudinal and vertical tire forces, respectively, without an explicit consideration of their interaction [3]. In such practice, conflicts between control objectives and execution effects arise. Realizing this, academic and industrial research communities become very active on studying integrated control to improve both comfort and safety on commercial cars [4,5].

Nevertheless, two problems persist during the design stage of a vehicle dynamic controller. First, vehicle dynamics system integrated control complicates the controller design. To reduce the complexity of the overall system, the integrated vehicle dynamics control system is divided into a vehicle motion controller and a tire force distributor, i.e., the vehicle longitudinal/vertical speed and pitch are controlled first, prior to the optimal control of the tire force. Second, the tire parameters become uncertain where the vehicle is on low-adhesion coefficient road or at high speeds. Therefore, the designed control system must behave robustly to

handle the uncertainties. In [6,7], the problem was solved for aerial vehicles based on sliding mode control (SMC). Therefore, SMC is expected to solve similar problems involving uncertain EV parameters.

Figure 1 shows the solutions adopted to address the two above mentioned problems. The proposed integrated vehicle dynamics controller regulates the total forces/moment distribution for each tire. According to the control requirements of speed tracking and the comfort performance, the vehicle is controlled to obtain the total longitudinal force, total vertical force, and total pitching moment. Furthermore, to ensure the safety and comfort of the vehicle, minimize-the-tire-load command is proposed in the optimal distribution of the tire force. The vehicle dynamics integrated control method is described in three steps.

Step 1. A vehicle dynamic model is created by considering the pitch, and longitudinal and vertical movement as expressed by

$$m_s(\dot{v}_x + v_z \cdot \dot{\theta}) = F_{x1} + F_{x2} + F_{x3} + F_{x4} - f_{\text{air}}, \quad (1)$$

where m_s is mass of the vehicle, v_x is longitudinal speed, v_z is vertical speed, and θ is pitch angle. F_{xi} , $i = 1, 2, 3, 4$ represent the tire longitudinal forces, f_{air} is the air resistance and $f_{\text{air}} = \frac{1}{2}\rho C_d A v_x^2$, ρ is the air density, C_d is the drag coefficient, and A is the vehicle windward area. More-

* Corresponding author (email: hyzhao2008@126.com)

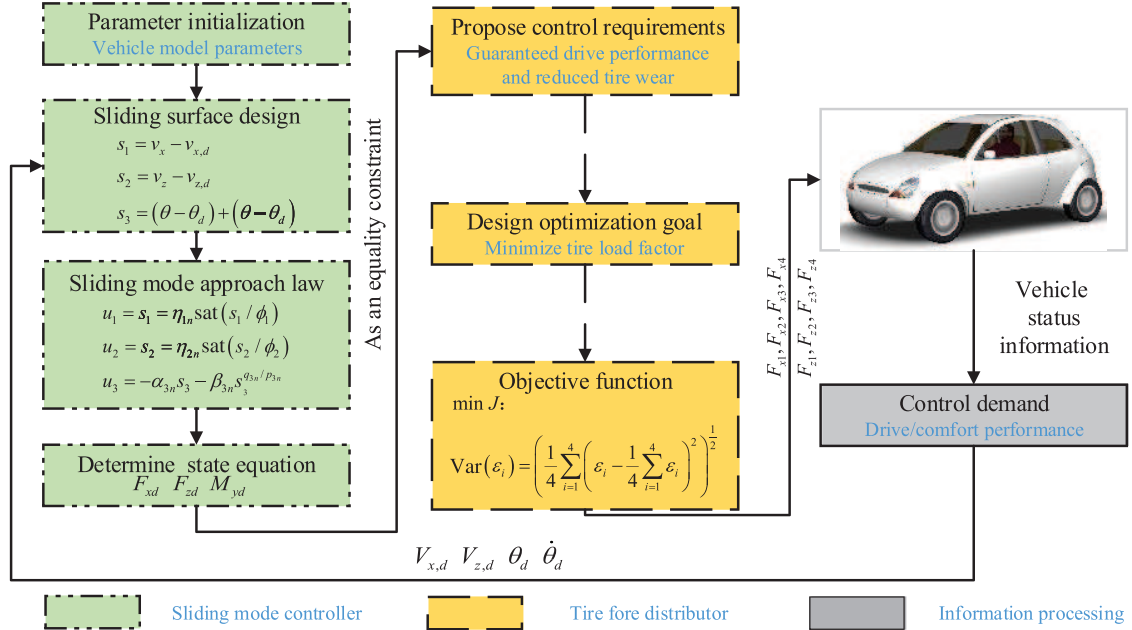


Figure 1 (Color online) Overall block diagram of vehicle longitudinal-vertical integrated control.

over,

$$m_s(\dot{v}_z - v_x \cdot \dot{\theta}) = F_{z1} + F_{z2} + F_{z3} + F_{z4} - m_s g, \quad (2)$$

where F_{zi} , $i = 1, 2, 3, 4$ represent the tire vertical forces and g is gravitational acceleration.

Correspondingly,

$$I_y \ddot{\theta} = -l_f(F_{z1} + F_{z2}) + l_r(F_{z3} + F_{z4}), \quad (3)$$

where I_y indicates the inertia of the pitch moment around the Y -axis (lateral axis), l_f and l_r are the front wheelbase and the rear wheelbase, respectively.

Step 2. The SMC motion controller is designed to output the longitudinal/vertical force and pitching moment of the vehicle.

The integrated vehicle dynamics control system focuses on tracking the longitudinal speed and comfort in the vertical speed. Therefore, these control targets are needed: $v_x = v_{x,d}$, $v_{z,d} = 0$, $\dot{\theta}_d = 0$, where $v_{x,d}$, $v_{z,d}$ are the desired longitudinal force and desired vertical force, separately. $\dot{\theta}_d$ is the desired pitch rate.

To track the longitudinal/vertical speed and pitch rate of the vehicle, three switching functions are selected:

$$\begin{aligned} s_1 &= v_x - v_{x,d}, \\ s_2 &= v_z - v_{z,d}, \\ s_3 &= (\theta - \theta_d) + (\dot{\theta} - \dot{\theta}_d). \end{aligned} \quad (4)$$

Sliding surfaces s_1 and s_2 are designed to ensure that longitudinal and vertical speeds track the desired speed. If the sliding surface s_3 is simplified to

the error tracking of the pitch rate, then the system will accumulate pitch errors. Therefore, the error of the pitch angle is considered in s_3 .

To weaken the phenomenon of chattering in SMC, the variable boundary saturation function approach law is adopted [8]. Combining the vehicle dynamics equation derived in Step 1 yields the desired longitudinal force defined by

$$F_{xd} = u_1 = m_s(v_z \cdot \dot{\theta} + \dot{v}_x - \dot{s}_1 - \eta_{1n} \text{sat}(s_1/\phi_1)) + \frac{1}{2} \rho C_d A v_x^2, \quad (5)$$

$$F_{zd} = u_2 = m_s(-v_x \cdot \dot{\theta} + \dot{v}_z - \dot{s}_2 - \eta_{2n} \text{sat}(s_2/\phi_2)) + mg. \quad (6)$$

$$M_{yd} = u_3 = I_y \left(-\frac{\alpha_{3n} s_3 + \beta_{3n} s_3^{q_{3n}/p_{3n}}}{\beta_{3n} p_3} \cdot q_3 \cdot \dot{\theta}^{1-p_3/q_3} - \frac{\alpha_3 q_3}{\beta_3 p_3} \cdot \dot{\theta}^{2-p_3/q_3} \right). \quad (7)$$

See Appendix A for the parameters of the vehicle and the sliding mode controller.

Step 3. This step aims to design the tire force distributor. The vertical dynamic coefficient of the tire is taken as the target for optimization of the tire force that subsequently improves the EV comfort performance.

An optimal longitudinal force distribution apportions the desired longitudinal force evenly to ensure its largest effective range. However, the change in vertical force directly affects the longitudinal force and comfort of the vehicle. To solve

this, the active vertical force of each tire is minimized as much as possible to ensure the driving posture of the vehicle, as follows:

$$\min J = \text{Var}(\varepsilon_i) = \left(\frac{1}{4} \sum_{i=1}^4 \left(\varepsilon_i - \frac{1}{4} \sum_{i=1}^4 \varepsilon_i \right)^2 \right)^{\frac{1}{2}}, \quad (8)$$

where ε_i indicates the vertical dynamic coefficient of the tire, calculated by

$$\begin{aligned} \varepsilon_i &= \frac{F_{zi,0}}{F_{zi}}, \\ F_{z1,0} = F_{z2,0} &= \frac{l_r}{2l} m_s g, \\ F_{z3,0} = F_{z4,0} &= \frac{l_f}{2l} m_s g, \end{aligned} \quad (9)$$

where $F_{zi,0}$ denotes the vertical force experienced by a stationary tire.

The tire force should satisfy the actual and dynamic constraints during the distribution process. The range of tire force in each wheel is limited by various constraints, such as the desired total force and moment constraints, tire adhesion limit constraints, and actuator characteristic constraints. Furthermore, the longitudinal tire force is subject to the performance of the actuator. For a four-wheel drive EV, the maximum tire longitudinal force cannot exceed the force provided by the hub motor. Additionally, the torque provided by the hub motor is not changed quickly due to the influence of its own mechanical properties. Similarly, the torque provided by the suspension motor is not changed quickly. The active vertical forces of all tires are not negative:

$$\begin{aligned} \min J &= \text{Var}(\varepsilon_i) = \left(\frac{1}{4} \sum_{i=1}^4 \left(\varepsilon_i - \frac{1}{4} \sum_{i=1}^4 \varepsilon_i \right)^2 \right)^{\frac{1}{2}} \\ \text{s.t. } F_{xd} &= F_{x1} + F_{x2} + F_{x3} + F_{x4}, \\ F_{zd} &= F_{z1} + F_{z2} + F_{z3} + F_{z4}, \\ M_{yd} &= -l_f (F_{z1} + F_{z2}) + l_r (F_{z3} + F_{z4}), \\ -T_{i,\max} &\leq F_{xi} \cdot r \leq T_{i,\max}, \\ -k_{xi,\max}/r &\leq \Delta F_{xi}/\Delta t \leq k_{xi,\max}/r, \\ F_{zi} &\geq 0, \\ -k_{zi,\max} &\leq \Delta F_{zi}/\Delta t \leq k_{zi,\max}, \end{aligned} \quad (10)$$

where $T_{i,\max}$, $i = 1, 2, 3, 4$ represents the maximum torque of each hub motor, r indicates the radius of the tire, $k_{xi,\max}$ denotes the hub motor torque maximum rate of change, ΔF_{xi} represents the magnitude change of the longitudinal tire force per unit time, $k_{zi,\max}$ indicates the maximum change rate of suspension motor torque, and ΔF_{zi} represents the magnitude change of the vertical tire force per unit time.

Conclusion. This study proposed the vehicle dynamics control system of the distributed EV, in which the complex problem of the vehicle's dynamic control is transformed into the longitudinal speed/ vertical speed/ pitch angle tracking control with an optimized tire force. With regard to the vehicle state and tire vertical dynamic coefficient, the tire force distributor improves the speed tracking performance. The presented nonlinear constraints consider the saturation constraint of the actuator, and pave the way for a subsequent actuator control. Therefore, the proposed control system exhibits tracking capability that is significantly improved in driving/braking performances at high speed.

Acknowledgements This work was supported by National Natural Science Foundation of China (Grant Nos. U1564207, U1664257), Industrial Innovation Special Funds of Jilin Province (Grant No. 2018C035-2), and Graduate Innovation Fund of Jilin University (Grant No. 419020391355).

Supporting information Appendixes A and B. The supporting information is available online at info.scichina.com and link.springer.com. The supporting materials are published as submitted, without typesetting or editing. The responsibility for scientific accuracy and content remains entirely with the authors.

References

- 1 Zeng X, Li G, Yin G, et al. Model predictive control-based dynamic coordinate strategy for hydraulic hub-motor auxiliary system of a heavy commercial vehicle. *Mech Syst Signal Process*, 2018, 101: 97–120
- 2 Zhao H Y, Ren B T, Chen H, et al. Model predictive control allocation for stability improvement of four-wheel drive electric vehicles in critical driving condition. *Control Theor Appl Iet*, 2015, 9: 2688–2696
- 3 Yu X, Liu L. Target enclosing and trajectory tracking for a mobile robot with input disturbances. *IEEE Control Syst Lett*, 2017, 1: 221–226
- 4 Yu Y, Yang Z, Han C, et al. Fuzzy adaptive backstepping sliding mode controller for high-precision deflection control of the magnetically suspended momentum wheel. *IEEE Trans Ind Electron*, 2018, 65: 3530–3538
- 5 Wang C, Zhao W, Luan Z, et al. Decoupling control of vehicle chassis system based on neural network inverse system. *Mech Syst Signal Process*, 2018, 106: 176–197
- 6 Pukdeboon C. Extended state observer-based third-order sliding mode finite-time attitude tracking controller for rigid spacecraft. *Sci China Inf Sci*, 2019, 62: 012206
- 7 Zhang Z, Wang F, Guo Y, et al. Multivariable sliding mode backstepping controller design for quadrotor UAV based on disturbance observer. *Sci China Inf Sci*, 2018, 61: 112207
- 8 Song P, Zong C, Tomizuka M. A terminal sliding mode based torque distribution control for an individual-wheel-drive vehicle. *J Zhejiang Univ Sci A*, 2014, 15: 681–693